

Noninvasive Visualization and Analysis of the Human Parafoveal Capillary Network Using Swept Source OCT Optical Microangiography

Laura Kuehlewein,^{1,2} Tudor C. Tepelus,^{1,2} Lin An,³ Mary K. Durbin,³ Sowmya Srinivas,^{1,2} and Srinivas R. Sadda^{1,2}

¹Doheny Eye Institute, Los Angeles, California, United States

²Department of Ophthalmology, Keck School of Medicine, University of Southern California, Los Angeles, California, United States

³Carl Zeiss Meditec, Inc., Dublin, California, United States

Correspondence: Srinivas R. Sadda, Doheny Eye Institute, 1450 San Pablo Street, Los Angeles, CA 90033, USA; SSadda@doheny.org.

Submitted: January 21, 2015

Accepted: March 15, 2015

Citation: Kuehlewein L, Tepelus TC, An L, Durbin MK, Srinivas S, Sadda SR. Noninvasive visualization and analysis of the human parafoveal capillary network using swept source OCT optical microangiography. *Invest Ophthalmol Vis Sci.* 2015;56:3984-3988. DOI:10.1167/iovs.15-16510

PURPOSE. We characterized the foveal avascular zone (FAZ) and the parafoveal capillary network in healthy subjects using swept source OCT optical microangiography (OMAG).

METHODS. We acquired OMAG images of the macula of 19 eyes (13 healthy individuals) using a prototype swept source laser OCT. En face images of the retinal vasculature were generated for superficial and deep inner retinal layers (SRL/DRL) in regions of interest 250 (ROI-250) and 500 (ROI-500) μm from the FAZ border.

RESULTS. The mean area (mm^2) of the FAZ was 0.304 ± 0.132 for the SRL and 0.486 ± 0.162 for the DRL ($P < 0.001$). Mean vessel density (%) was 67.3 ± 6.4 for the SRL and 34.5 ± 8.6 for the DRL in the ROI-250 ($P < 0.001$), and 74.2 ± 3.9 for the SRL and 72.3 ± 4.9 for the DRL in the ROI-500 ($P = 0.160$).

CONCLUSIONS. Swept source OMAG images of healthy subjects allowed analysis of the FAZ and the density of the parafoveal capillary network at different retinal layers.

Keywords: optical coherence tomography, angiography, image analysis, fovea, parafoveal capillaries

The fovea is the source of highest resolution vision. Its histological structure differs from the rest of the retina, with its inner retinal layers, including the capillaries, displaced from the photoreceptors to form the foveal avascular zone (FAZ).¹ The FAZ is surrounded by a terminal capillary ring of side-branching retinal arterioles originating from the superior and inferior temporal branches of the central retinal artery.² Elsewhere in the retina, capillary networks originating from the central retinal artery are located in different layers of the inner retina.^{3,4} The parafoveal capillary network and FAZ have been studied in vitro and in vivo, using various methods, including histologic techniques, high contrast entoptic view, fluorescein angiography (FA), and high-resolution imaging tools, such as adaptive optics and confocal scanning laser ophthalmoscopy.⁵⁻¹³ The introduction of phase variance optical coherence tomography (OCT) made it possible to visualize the retinal vasculature, including the capillaries with OCT technology.¹⁴ In particular, swept source (SS) ultrahigh-speed frequency domain OCT optical microangiography (OMAG) provides simultaneously high-resolution and three-dimensional information on the morphology of the retinal vasculature by capturing a series of B-scans in the same location, allowing isolation of motion (blood flow) signals from static (tissue) signals by image processing.¹⁵ The OMAG technique is a noninvasive, comfortable imaging method for the patient.

In the present study, we applied this novel, noninvasive imaging modality to characterize the FAZ and parafoveal capillary network in healthy subjects, and to compare our findings to those of previous studies on capillary visualization.

PATIENTS AND METHODS

A total of 13 healthy subjects participated in this study. Exclusion criteria included any evidence of ocular pathology or systemic disease. Informed consent was obtained from all subjects. The study protocol was approved by the Health Science Institutional Review Board of the University of Southern California and complied with the requirements of the Declaration of Helsinki.

Swept source OMAG images were acquired using a prototype SS laser OCT (510K clearance pending) from Carl Zeiss Meditec (Dublin, CA, USA) with a central wavelength of 1050 nm (1000-1100 nm full width), a speed of 100,000 A-scans per second, and a theoretical axial and transverse resolution of 5 and 15 μm in tissue. For SS-OMAG imaging, $3 \times 3 \times 3$ mm macular cubes were acquired, with each cube consisting of 300 clusters of four repeated B-scans, each containing 300 A-scans. The time to acquire one cube was approximately 4.5 seconds. Clusters of four B-scans were taken to enable the visualization of motion when generating SS-OMAG images. An intensity differentiation algorithm was applied to extract in vivo blood vessel information as described previously.¹⁶ Before the algorithm was applied, displacement occurring between adjacent repeated B-scans caused by involuntary eye movement was compensated by a two-dimensional cross correlation between two adjacent flow images.¹⁷ Using this approach, we obtained detailed, depth-resolved images of the retinal vasculature in the posterior pole.

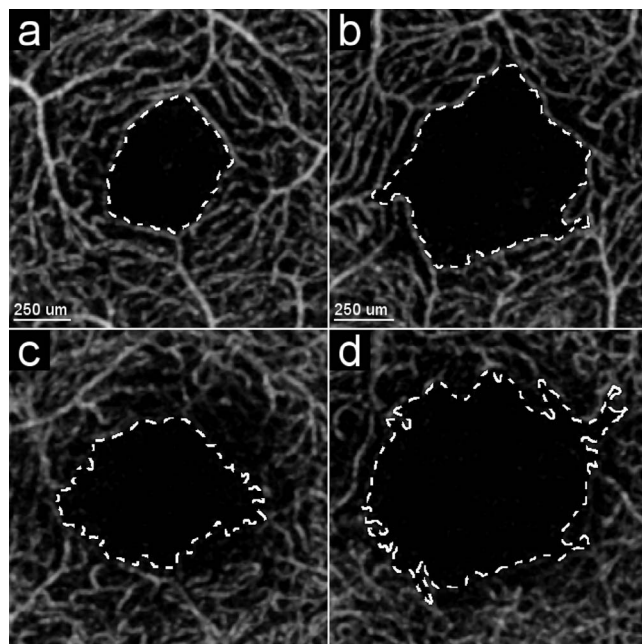


FIGURE 1. Swept source OCT optical microangiography images of two subjects centered on the fovea. (a, b) En face projection image of the FAZ (outlined) and the parafoveal microvasculature of the SRL. (c, d) Corresponding en face projection images of the DRL.

To delineate the best plane to separate the superficial and deep retinal capillaries, we first generated a rough estimate of the position of the outer border of the outer plexiform layer as approximately 110 μm internal to the retinal pigment epithelium. The automated algorithms used to estimate the position were based on existing segmentation techniques used in the Cirrus OCT (Carl Zeiss Meditec) to identify the retinal pigment epithelium and inner limiting membrane in the OCT intensity image.¹⁸ The neurosensory retina internal to this boundary was designated the inner retina and was divided further empirically into superficial (inner 60%) and deep (outer 40%) retinal capillary layers (SRL/DRL). En face images of the retinal vasculature were generated by a maximum intensity projection for the two identified layers. Generating the en face images took less than 10 seconds per cube.

Quantitative analyses were performed using the publically available GNU Image Manipulation Program GIMP 2.8.14 (available in the public domain at <http://gimp.org>). First, the area of the FAZ, defined by the area inside the inner border of the terminal capillary ring, was semiautomatically delineated by two independent graders for the SRL and DRL images (Fig. 1). Measures in pixels were converted to millimeters with respect to the axial length (assessed with the IOL-Master; Carl Zeiss Meditec) to correct for individual differences in ocular magnification as reported previously.¹⁹ The effective diameter of the FAZ was calculated as the diameter of a circle with equal area ($D_{\text{eff}} = 2\sqrt{[\text{Area}/\pi]}$).

Two regions of interest (ROI) surrounding the FAZ, from the border of the FAZ to a distance of 250 μm from the border of the FAZ, and from a distance of 250 μm to a distance of 500 μm from the border of the FAZ as determined on the SRL image, were extracted from the SRL and DRL images of each eye using the layer projection, selection and expand selection tools of GIMP. The distance of 250 μm (ROI-250) was chosen because inspection of the images revealed that, on the SRL images, the vessels were easiest to distinguish within this distance of the terminal capillary ring. The second distance of 500 μm (ROI-

500) was chosen based on the histologic definition of the parafoveal region.²⁰ In a last step, the vessels visible in the ROI were extracted semiautomatically with the color selection tool of GIMP for further analysis (Fig. 2). Vessel density was assessed as percent of retinal area occupied by vessels.

Statistical analyses were performed with PASW Statistics for Windows, Version 18.0 (SPSS, Inc., Chicago, IL, USA) using the Shapiro-Wilk test for normality and the paired samples *t*-test to determine differences when comparing matched samples in normally distributed populations. Intraclass correlation coefficients with 95% confidence intervals were calculated to assess intergrader agreement. The significance level was set at 5%.

Of the 13 participants, 8 were male, 5 female. The age range was 26 to 41 years, with a mean of 31 and an SD of 5 years. In six subjects, in whom both eyes were imaged, the measures were averaged for the right and left eyes.

RESULTS

The mean (SD) axial length was 24.33 (0.92) mm.

Side-by-side inspection of images extracted from the SRL and DRL showed fewer visible vessels overall and larger central avascular areas for the DRL (Fig. 1). Table 1 shows the mean (SD) of the area and effective diameter of the FAZ, and the vessel density in the ROI for the SRL and DRL.

The mean size and effective diameter of the FAZ were statistically significantly smaller in the SRL compared to the DRL. The mean (SD) and percent differences were 0.182 (0.058) mm^2 and 48.9% (18.2%), respectively, for the area of the FAZ, and 0.095 (0.029) mm and 25.0% (10.0%) for the effective diameter (paired *t*-test, $P < 0.001$). Measurements of the FAZ size were highly correlated between the two graders with intraclass correlation coefficients (95% confidence interval) of 0.982 (0.938–0.994) for the SRL and 0.856 (0.668–0.942) for the DRL. The mean \pm SD and absolute

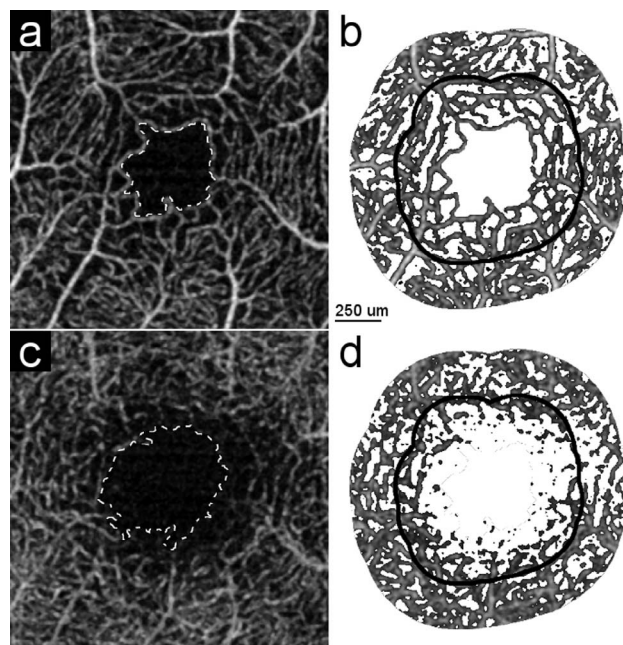


FIGURE 2. Side-by-side comparison of en face projection and vessel extraction images of the SRL and DRL of the same eye. (a, c) En face projection image of the parafoveal vasculature of the SRL/DRL. The dashed white line shows the boundary of the FAZ. (b, d) Corresponding vessel extraction image of the SRL and DRL. The black outline shows the border between the ROI-250 and ROI-500.

TABLE 1. Mean (SD) Area and Effective Diameter of the FAZ and Vessel Density in Percent Retinal Area Occupied by Vessels for ROI With a Distance of 250 and 500 μm From the Terminal Capillary Ring of the FAZ

	Superficial Inner Retinal Layer	Deep Inner Retinal Layer
FAZ area, mm^2	0.304 (0.132)	0.486 (0.162)
FAZ effective diameter, mm	0.344 (0.074)	0.438 (0.072)
Vessel density ROI-250, %	67.3 (6.4)	34.5 (8.6)
Vessel density ROI-500, %	74.2 (3.9)	72.3 (4.9)

mean differences in FAZ area measurements between the two graders were -0.013 ± 0.020 and $0.014 \pm 0.019 \text{ mm}^2$ for the SRL, and 0.014 ± 0.086 and $0.060 \pm 0.062 \text{ mm}^2$ for the DRL.

The mean vessel density in the ROI-250 was statistically significantly greater in the SRL. The mean (SD) percent difference in vessel density was 32.8 (9.3, paired *t*-test, $P < 0.001$). In the ROI-500, there was no statistically significant difference in the mean vessel density when comparing the SRL and DRL (paired *t*-test, $P = 0.160$). The corresponding boxplot is shown in Figure 3.

DISCUSSION

Ultrahigh-speed SS-OMAG can be used to produce detailed en face in vivo images of the FAZ and parafoveal vascular network noninvasively at different layers of the retina, suggesting that this technique may be used to study the vasculature of the central retina in healthy and diseased eyes.

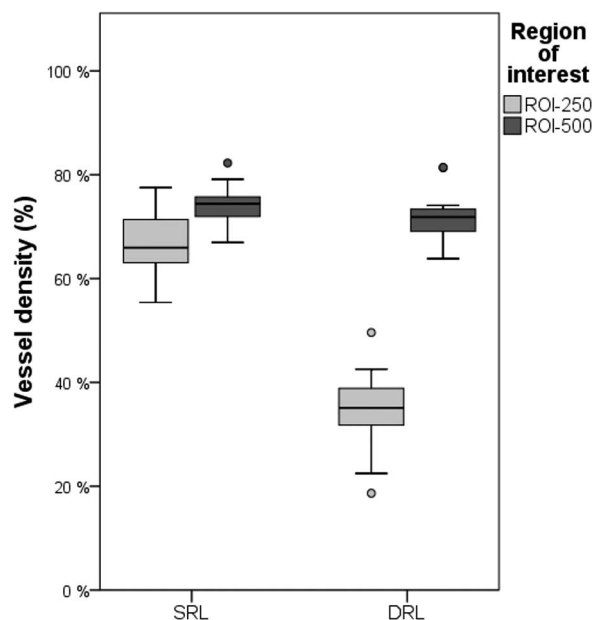
The mean FAZ area and effective diameter in normal subjects corrected for axial length in this study (0.304 mm^2 and 0.344 mm for the SRL) were similar to results from previous studies using different modalities as shown in Table 2.

Parafoveal vessel density has been reported for regions resembling our ROI-250 and ROI-500 in previous studies. For

TABLE 2. Size of the FAZ in Healthy Subjects From Present and Other Studies

Technique	N	FAZ, mm^2
Retinal function imager ²³	37	0.125 ± 0.070
High-speed phase-variance OCT ¹⁴	2	0.167
Scanning laser ophthalmoscope FA ²⁴	52	0.205 ± 0.060
Scanning laser ophthalmoscope FA ²⁵	21	0.231 ± 0.060
Contrast-adjusted scanning laser ophthalmoscope FA ⁹	31	0.275 ± 0.074
High-resolution, wide-field, dual-conjugate adaptive optics ¹³	5	0.302 ± 0.100
Present study: swept source OMAG	13	$0.304 (0.132)$
Adaptive optics scanning laser ophthalmoscope ¹⁰	10	0.323 ± 0.107
Adaptive optics scanning laser ophthalmoscope ¹¹	11	0.330 ± 0.190
FA ²⁶	20	0.35
FA ²⁷	27	0.405
Retinal function imager, scanning laser ophthalmoscope, FA ¹²	42	0.420 ± 0.250
High contrast entoptic view ⁶	34	0.42

example, using an adaptive optics scanning laser ophthalmoscope, Tam et al.¹⁰ found an average vessel density of 31.6 mm^{-1} ($N = 10$) in the inner region. In addition, using a high-resolution, wide-field dual-conjugate adaptive optics instrument, Popovic et al.¹³ found a mean capillary density of 38.0 mm^{-1} in the inner ROI, and 36.4 mm^{-1} in the outer ROI ($N = 5$). In both studies, measurements were corrected for ocular magnification. In a histologic study, Mendis et al.⁴ found a mean vessel density of 41.1% in the superficial and 23.0% in the deep capillary network in confocal microscopy ($N = 5$). The specimens, however, were taken at 850 to 2150 μm eccentricity from the foveal center. With FA, they found a mean vessel density of 24.4% in the same location ($N = 10$).⁴ To convert their numbers to measures similar to those used by Tam et al.¹⁰ and Popovic et al.¹³, we could assume a capillary width of 7 μm . Their "capillary percent area" yields an area measurement that can be divided by capillary width to obtain total capillary length. Dividing total capillary length by the area of the ROI yields a metric that can be compared to other studies. Applying this algorithm, the measurements of Mendis et al.⁴ convert to 58.6 and 32.9 mm^{-1} in the superficial and deep layer by confocal microscopy, and 34.3 mm^{-1} by FA. Our measures can be similarly converted using an estimated capillary width of 15 μm to account for the apparent wider appearance of capillaries on OCT imaging. On our first assessment of the data, based on multiple measurements of the parafoveal capillaries in several images/cases, the average width appeared to be 15 μm , which corresponds to the transverse resolution of the SS-OCT system. Thus, based on the optical limitations, the use of an estimated capillary width of 15 μm for our study appears appropriate. Using this assumption, our mean capillary density in the SRL converts to 44.9 mm^{-1} in the ROI-250 and 49.5 mm^{-1} in the ROI-500. In the DRL, the mean capillary density converts to 23.0 mm^{-1} in the ROI-250 and 48.2 mm^{-1} in the ROI-500. When compared to the results of Tam et al.¹⁰ and Popovic et al.,¹³ our estimated vessel density is higher. This is most likely due to the different vessel extraction technique: Tam et al.¹⁰ outlined the centerlines of the vessels, and Popovic et al.¹³ skeletonized the vessel signature to a 1 pixel-wide tracing. In this study, the extracted vessel signature was not skeletonized as shown in Figure 2. When compared to the results of Mendis et al.,⁴ our estimated vessel density is lower for the superficial inner retinal layer.

**FIGURE 3.** Boxplot showing the vessel density in percent retinal area occupied by vessels for the ROI in the SRL and DRL. The ROI-250 was defined as the area within a distance of 250 μm from the terminal capillary ring; the ROI-500 was defined as the area outside the ROI-250 within a distance of 500 μm from the terminal capillary ring.

This was expected as the specimens of Mendis et al.⁴ were taken at a greater eccentricity. Recently, Chui et al.²¹ used adaptive optics scanning laser ophthalmoscope imaging to study the relationship between the thickness of the retina and size of FAZ, and suggested that the inner retinal circulation might be required to support a retinal thickness greater than 60 μm .²¹ It would be interesting in the future with a larger cohort to determine whether a similar relationship could be established between retinal thickness and the OMAG determined FAZ.

Although the methods we used have many advantages, including the rapid and comfortable acquisition of the OMAG images, the depth resolution, excellent microvascular resolution, and the semiautomated analysis technique, there are several limitations to consider. These drawbacks include rare motion artifacts, low edge contrast of the vessels on the images, and the subjectivity of some of the assessments when determining vessel borders. Motion artifacts could be addressed by including faster eye-tracking to improve the image quality, especially in subjects with poor fixation/reduced visual acuity. The edge contrast limitation could be overcome by optimizing the postimage processing algorithms.⁴ An enhanced edge contrast of the vessels would likely increase the reliability of the measurements by facilitating the vessel border selection. With further improvements, a three-dimensional display and analysis of the vessel structure would make it possible to assess the vessel density proportional to the volume evaluated. A three-dimensional approach to study the vasculature is particularly important, since the division of the parafoveal capillaries into superficial and deep layers by OMAG imaging is somewhat arbitrary.

In summary, the FAZ and parafoveal capillary networks can be visualized noninvasively, three-dimensionally, and with high resolution using ultrahigh-speed SS-OMAG. In the present study, images acquired with this technique in healthy subjects allowed analysis of the FAZ and density of the parafoveal capillary network at different retinal layers. Selective visualization of the deep retinal capillary plexus, which cannot be accomplished by FA, is of particular interest as recent reports have identified diseases featuring isolated deep capillary ischemia.²² This suggests that this technique may be of great value to study the vasculature of the central retina in healthy and diseased eyes.

Acknowledgments

Supported by Carl Zeiss Meditec, Optos, and Allergan (SRS). The authors alone are responsible for the content and writing of the paper.

Disclosure: **L. Kuehlewein**, None; **T.C. Tepelus**, None; **L. An**, Carl Zeiss Meditec (E); **M.K. Durbin**, Carl Zeiss Meditec (E); **S. Srinivas**, None; **S.R. Sadda**, Carl Zeiss Meditec (F, C, R), Optos (E, C, R), Allergan (F, C, R), Genentech (C), Alcon (C); Novartis (C); Roche (C), Heidelberg Engineering (S), P

References

- Provis JM, Dubis AM, Maddess T, Carroll J. Adaptation of the central retina for high acuity vision: cones, the fovea and the avascular zone. *Prog Retin Eye Res.* 2013;35:63-81.
- Anderson B Jr, McIntosh HD. Retinal circulation. *Annu Rev Med.* 1967;18:15-26.
- Tan PE, Yu PK, Balaratnasingam C, et al. Quantitative confocal imaging of the retinal microvasculature in the human retina. *Invest Ophthalmol Vis Sci.* 2012;53:5728-5736.
- Mendis KR, Balaratnasingam C, Yu P, et al. Correlation of histologic and clinical images to determine the diagnostic value of fluorescein angiography for studying retinal capillary detail. *Invest Ophthalmol Vis Sci.* 2010;51:5864-5869.
- Provis JM, Hendrickson AE. The foveal avascular region of developing human retina. *Arch Ophthalmol.* 2008;126:507-511.
- Bradley A, Applegate RA, Zeffren BS, van Heuven WA. Psychophysical measurement of the size and shape of the human foveal avascular zone. *Ophthalmic Physiol Opt.* 1992; 12:18-23.
- Weinhaus RS, Burke JM, Delori FC, Snodderly DM. Comparison of fluorescein angiography with microvascular anatomy of macaque retinas. *Exp Eye Res.* 1995;61:1-16.
- Zheng Y, Gandhi JS, Stangos AN, Campa C, Broadbent DM, Harding SP. Automated segmentation of foveal avascular zone in fundus fluorescein angiography. *Invest Ophthalmol Vis Sci.* 2010;51:3653-3659.
- John D, Kuriakose T, Devasahayam S, Braganza A. Dimensions of the foveal avascular zone using the Heidelberg retinal angiogram-2 in normal eyes. *Indian J Ophthalmol.* 2011;59:9-11.
- Tam J, Martin JA, Roorda A. Noninvasive visualization and analysis of parafoveal capillaries in humans. *Invest Ophthalmol Vis Sci.* 2010;51:1691-1698.
- Chui TY, Zhong Z, Song H, Burns SA. Foveal avascular zone and its relationship to foveal pit shape. *Optom Vis Sci.* 2012; 89:602-610.
- Dubis AM, Hansen BR, Cooper RE, Beringer J, Durbra A, Carroll J. Relationship between the foveal avascular zone and foveal pit morphology. *Invest Ophthalmol Vis Sci.* 2012;53:1628-1636.
- Popovic Z, Knutsson P, Thaug J, Owner-Petersen M, Sjöstrand J. Noninvasive imaging of human foveal capillary network using dual-conjugate adaptive optics. *Invest Ophthalmol Vis Sci.* 2011;52:2649-2655.
- Kim DY, Fingler J, Zawadzki RJ, et al. Noninvasive imaging of the foveal avascular zone with high-speed, phase-variance optical coherence tomography. *Invest Ophthalmol Vis Sci.* 2012;53:85-92.
- An L, Shen TT, Wang RK. Using ultrahigh sensitive optical microangiography to achieve comprehensive depth resolved microvasculature mapping for human retina. *J Biomed Opt.* 2011;16:106013.
- Huang Y, Zhang Q, Thorell MR, et al. Swept-source OCT angiography of the retinal vasculature using intensity differentiation-based optical microangiography algorithms. *Ophthalmic Surg Lasers Imaging Retina.* 2014;45:382-389.
- An L, Subhush HM, Wilson DJ, Wang RK. High-resolution wide-field imaging of retinal and choroidal blood perfusion with optical microangiography. *J Biomed Opt.* 2010;15:026011.
- Bagci AM, Shahidi M, Ansari R, Blair M, Blair NP, Zelkha R. Thickness profiles of retinal layers by optical coherence tomography image segmentation. *Am J Ophthalmol.* 2008; 146:679-687.
- Bennett AG, Rudnicka AR, Edgar DF. Improvements on Littmann's method of determining the size of retinal features by fundus photography. *Graefes Arch Clin Exp Ophthalmol.* 1994;32:361-367.
- Regillo C. *Basic and Clinical Science Course: Section 12, Retina and Vitreous, 2008-2009.* San Francisco, CA: American Academy of Ophthalmology; 2008:10.
- Chui TY, VanNasdale DA, Elsner AE, Burns SA. The association between the foveal avascular zone and retinal thickness. *Invest Ophthalmol Vis Sci.* 2014;55:6870-6877.
- Sarraf D, Rahimy E, Fawzi AA, et al. Paracentral acute middle maculopathy: a new variant of acute macular neuroretinopathy associated with retinal capillary ischemia. *JAMA Ophthalmol.* 2013;131:1275-1287.

23. Nelson DA, Burgansky-Eliash Z, Barash H, et al. High-resolution wide-field imaging of perfused capillaries without the use of contrast agent. *Clin Ophthalmol*. 2011;5:1095-1106.
24. Arend O, Wolf S, Harris A, Reim M. The relationship of macular microcirculation to visual acuity in diabetic patients. *Arch Ophthalmol*. 1995;113:610-614.
25. Arend O, Wolf S, Jung F, et al. Retinal microcirculation in patients with diabetes mellitus: dynamic and morphological analysis of perifoveal capillary network. *Br J Ophthalmol*. 1991;75:514-518.
26. Bresnick GH, Condit R, Syrjala S, Palta M, Groo A, Korth K. Abnormalities of the foveal avascular zone in diabetic retinopathy. *Arch Ophthalmol*. 1984;102:1286-1293.
27. Mansour AM, Schachat A, Bodiford G, Haymond R. Foveal avascular zone in diabetes mellitus. *Retina*. 1993;13:125-128.